

Selective Glucocorticoid Receptor Modulation Prevents and Reverses Nonalcoholic Fatty Liver Disease in Male Mice

Lisa L. Koorneef,^{1,2*} José K. van den Heuvel,^{1,2*} Jan Kroon,^{1,2} Mariëtte R. Boon,^{1,2} Peter A. C. 't Hoen,^{3,4} Kristina M. Hettne,³ Nienke M. van de Velde,^{1,2} Kelsey B. Kolenbrander,^{1,2} Trea C. M. Streefland,^{1,2} Isabel M. Mol,^{1,2} Hetty C. M. Sips,^{1,2} Szymon M. Kielbasa,⁵ Hailiang Mei,⁶ Joseph K. Belanoff,⁷ Alberto M. Pereira,¹ Maaike H. Oosterveer,^{8,9} Hazel Hunt,⁷ Patrick C. N. Rensen,^{1,2} and Onno C. Meijer^{1,2}

¹Department of Internal Medicine, Division of Endocrinology, Leiden University Medical Center, 2333 ZA Leiden, Netherlands; ²Eindhoven Laboratory for Experimental Vascular Medicine, Leiden University Medical Center, 2333 ZA Leiden, Netherlands; ³Department of Human Genetics, Leiden University Medical Center, 2333 ZA Leiden, Netherlands; ⁴Centre for Molecular and Biomolecular Informatics, Radboud Institute for Molecular Life Sciences, Radboud University Medical Center Nijmegen, 6525 GA Nijmegen, Netherlands; ⁵Bioinformatics Center for Expertise, Leiden University Medical Center, 2333 ZA Leiden, Netherlands; ⁶Sequencing Analysis Support Core, Leiden University Medical Center, 2333 ZA Leiden, Netherlands; ⁷Concept Therapeutics, Menlo Park, California 94025; ⁸Department of Pediatrics, University of Groningen, University Medical Center Groningen, 9713 GZ Groningen, Netherlands; and ⁹Center for Liver Digestive and Metabolic Diseases, University of Groningen, University Medical Center Groningen, 9713 GZ Groningen, Netherlands

ORCID numbers: 0000-0002-1130-227X (L. L. Koorneef); 0000-0001-5656-3898 (J. Kroon); 0000-0002-4182-7560 (K. M. Hettne); 0000-0002-1194-9866 (A. M. Pereira); 0000-0003-4117-7833 (M. H. Oosterveer); 0000-0002-8455-4988 (P. C. N. Rensen); 0000-0002-8394-6859 (O. C. Meijer).

Medication for nonalcoholic fatty liver disease (NAFLD) is an unmet need. Glucocorticoid (GC) stress hormones drive fat metabolism in the liver, but both full blockade and full stimulation of GC signaling aggravate NAFLD pathology. We investigated the efficacy of selective glucocorticoid receptor (GR) modulator CORT118335, which recapitulates only a subset of GC actions, in reducing liver lipid accumulation in mice. Male C57BL/6J mice received a low-fat diet or high-fat diet mixed with vehicle or CORT118335. Livers were analyzed histologically and for genome-wide mRNA expression. Functionally, hepatic long-chain fatty acid (LCFA) composition was determined by gas chromatography. We determined very-low-density lipoprotein (VLDL) production by treatment with a lipoprotein lipase inhibitor after which blood was collected to isolate radiolabeled VLDL particles and apoB proteins. CORT118335 strongly prevented and reversed hepatic lipid accumulation. Liver transcriptome analysis showed increased expression of GR target genes involved in VLDL production. Accordingly, CORT118335 led to increased lipidation of VLDL particles, mimicking physiological GC action. Independent pathway analysis revealed that CORT118335 lacked induction of GC-responsive genes involved in cholesterol synthesis and LCFA uptake, which was indeed reflected in unaltered hepatic LCFA uptake *in vivo*. Our data thus reveal that the robust hepatic lipid-lowering effect of CORT118335 is due to a unique combination of GR-dependent stimulation of lipid (VLDL) efflux from the liver, with a lack of stimulation of GR-dependent hepatic fatty acid uptake. Our findings firmly demonstrate the potential use of CORT118335 in the treatment of NAFLD and underscore the potential of selective GR modulation in metabolic disease. (*Endocrinology* 159: 3925–3936, 2018)

Nonalcoholic fatty liver disease (NAFLD) is a prevalent condition (20% to 30% of the general population) with rising incidence due to the obesity pandemic; to date, long-term treatment options are restricted to weight loss surgery (1, 2). NAFLD can advance to non-alcoholic steatohepatitis and further progress toward hepatic fibrosis, cirrhosis, and hepatocellular carcinoma (3). NAFLD is caused primarily by an imbalance of hepatic energy influx and efflux. Because glucocorticoid (GC) hormones have a strong effect on hepatic energy homeostasis, modulation of GC signaling seems to be an interesting treatment option (4).

GCs (predominantly cortisol in humans and corticosterone in rodents) are secreted by the adrenal cortex during stress, mainly to support recruitment of energy reserves for the organism, and follow a diurnal rhythm. These effects are mediated by the glucocorticoid receptor (GR), a member of the nuclear receptor superfamily (5). Among the widespread effects of GCs are the regulation of metabolic pathways in the liver, including the stimulation of both hepatic *influx* (uptake of free fatty acids and lipoproteins and via *de novo* lipogenesis) and *efflux* of lipids [via very-low-density lipoprotein (VLDL) production] (6, 7). Because GCs control distinct pathways that induce and prevent steatosis, both excessive GC exposure and GR antagonism can promote development of liver steatosis and fibrosis (8, 9).

Selective GR modulators combine GR agonism and antagonism that, upon binding to GRs, induce unique receptor conformations that allow interaction with only subsets of downstream signaling pathways. Therapeutic potential has long been recognized for inflammatory disease, but unequivocal *in vivo* data remain limited, in particular in clinical settings (10–12). CORT118335 is a selective modulator that induces a profile of GR-coregulator interactions intermediate to full agonists and antagonists (13–15). In the current study, we demonstrated that CORT118335 fully prevents and reverses hepatic lipid accumulation in high-fat diet (HFD)–fed mice, highlighting the promise of selective GR modulation in metabolic disease.

Materials and Methods

Animal handling

The institutional ethics committee on animal care and experimentation at the Leiden University Medical Center approved all animal experiments that were conducted in Leiden (DEC13087 and DEC14245). Experiments were performed in 8-week-old male C57Bl/6J mice (Charles River Laboratories, St. Germain Nuelles, France). Mice were individually housed in conventional cages with a 12-hour:12-hour light-dark cycle with *ad libitum* access to food and water. Throughout metabolic experiments, body weight was determined twice a week

and body composition was monitored weekly using EchoMRI™ (Frankfurt, Germany).

To investigate the metabolic effects of CORT118335, mice were randomized according to body weight to receive a synthetic low-fat diet (LFD) or 10% fructose water with an HFD (60% lard; Research Diets, New Brunswick, NJ) containing vehicle, CORT118335 (60 mg/kg/d; Corcept Therapeutics, Menlo Park, CA), dexamethasone (1 mg/kg/d; Sigma-Aldrich, Zwijndrecht, Netherlands), or mifepristone (60 mg/kg/d; Corcept Therapeutics). To evaluate the efficacy of CORT118335 in a more severe NAFLD model with noncontinuous drug administration, mice received a 16-week run-in HFD (45% lard; Research Diets), after which they were randomized according to body weight to a 3-week oral gavage treatment with vehicle or CORT118335. Because peak drug levels are higher with oral administration, drug doses were decreased to 5 and 30 mg/kg/d. This study was carried out at RenaSci (Nottingham, United Kingdom).

For RNA sequencing and determination of hepatic lipid composition, mice received an LFD, HFD supplemented with vehicle, CORT118335 (60 mg/kg/d), or corticosterone (10 mg/kg/d) for 2 days (n = 4 per group). The rationale for the higher dose of CORT118335 was our hypothesis that part of its beneficial effects would depend on GR antagonism, requiring full receptor occupancy, whereas the dose of 10 mg/kg/d for corticosterone suffices for substantial agonist effects. For all experiments, mice were euthanized by cervical dislocation and perfused with ice-cold PBS, after which tissues were collected for further analysis.

Indirect calorimetry

At the start of the diet intervention, mice were transferred into fully automated metabolic cages for indirect calorimetry measurements (LabMaster System; TSE Systems, Bad Homburg, Germany). After 20 hours of acclimatization, oxygen consumption, carbon dioxide production, and caloric intake were measured for 5 consecutive days. Carbohydrate and fat oxidation rates and total energy expenditure were calculated from oxygen consumption and carbon dioxide production as described previously (16).

Intravenous glucose tolerance test

Mice were fasted for 6 hours before the experiment. At t = 0, blood was collected to measure basal plasma glucose, triglyceride (TG), and total cholesterol (TC) levels. Next, a glucose bolus was injected (2 g/kg), and at t = 5, t = 15, t = 30, t = 60, and t = 120 minutes, tail blood was collected and plasma glucose levels were measured (InstruChemie, Delfzijl, Netherlands).

Corticosterone and ACTH measurements

Basal plasma corticosterone and ACTH levels were measured in blood that was collected within 60 or 120 seconds after tail incision [*i.e.*, before ACTH and corticosterone levels, respectively, rose in the AM (8:00) and PM (18:00)]. During the novelty stress test, at t = 0 a blood sample was collected, after which mice were placed into a cage without bedding. After 10 minutes, a blood sample was collected, after which mice were placed back into their original home cage, and additional stress-free blood samples were collected at t = 30, t = 60, and t = 120 minutes. Plasma corticosterone levels were determined using ¹²⁵I RIA kits (MP Biochemicals, Amsterdam, Netherlands),

with 25 ng/mL as the lowest detection limit and coefficients of variation of <20%. Plasma ACTH levels were determined using the Double Antibody hACTH ¹²⁵I RIA kit (MP Biomedicals, Amsterdam, Netherlands), with 7 pg/mL as the lowest detection limit and coefficients of variation of <20%.

VLDL production measurement

Mice were fasted for 4 hours and subsequently anesthetized with 6.25 mg/kg acepromazine (Alfasan, Woerden, Netherlands), 6.25 mg/kg midazolam (Roche, Almere, Netherlands), and 0.31 mg/kg fentanyl (Janssen-Cilag, Breda, Netherlands). At $t = -30$ minutes, 20 μ Ci Tran³⁵SLABEL (S-35 methionine; MP Biomedicals) was injected into the tail vein. At $t = 0$, the lipoprotein lipase inhibitor Triton WR 1339 (0.5 g/kg; tyloxapol; Sigma-Aldrich) was additionally intravenously injected. At $t = 0, 15, 30, 60,$ and 90 minutes, blood was collected from the tail vein, and at $t = 120$ minutes, mice were exsanguinated via the orbital sinus and euthanized with an overdose of anesthesia. VLDL was isolated from serum after density gradient ultracentrifugation at $d < 1.006$ g/mL by aspiration (17). ApoB proteins were next isolated by precipitation with isopropanol and examined for incorporated ³⁵S activity.

Hepatic lipid determination with Cobas C111 analyzer

To extract lipids, HPLC-grade isopropanol (Fisher) was added to liver samples (1 mL/100 mg of tissue). To dissolve lipids, tissues were homogenized, vortexed, and incubated at 70°C for 25 minutes. Tubes were revortexed and centrifuged to remove undissolved matter, and the supernatant was assayed for TGs and TC using the Cobas C111 clinical analyzer (Roche) and associated reagents. The concentration of liver lipids was expressed as the concentration in the original tissue by multiplying by 10 as the liver sample was extracted in 10 volumes of isopropanol.

Hepatic lipid determination

Lipids were extracted from livers according to a modified protocol from Bligh and Dyer (18). Liver samples were homogenized in ice-cold methanol, and lipids were extracted into an organic phase (methanol/chloroform = 3:1). After centrifugation, the lower organic phase was dried and suspended in 2% Triton X-100 (Sigma-Aldrich). Hepatic TG and TC concentrations were measured using commercial enzymatic kits (Roche). Liver lipids were reported per milligram of protein, as determined using the bicinchoninic acid protein assay kit (Thermo Scientific, Rockford, IL).

Hepatic long-chain fatty acid determination

Frozen liver tissue was homogenized in PBS, and fatty acids were transmethylated to quantify fatty acid composition by gas chromatography using C17:0 as the internal standard (19).

Plasma lipid determination

Blood was collected in paraoxon-coated capillaries (Sigma-Aldrich), and TG, TC, and phospholipid content was measured using commercially available enzymatic kits for TG and TC (Roche) and phospholipid (InstruChemie).

Lipoprotein profiles

To determine the distribution of cholesterol and TGs over the various lipoproteins, pooled plasma samples ($n = 8$ per pool) were used for fast-performance liquid chromatography. Plasma was injected onto a Superose 6 column (Äkta system; Amersham Pharmacia Biotech, Kent, United Kingdom) and eluted at a constant flow rate (50 μ L/min) with PBS (pH, 7.4). In the collected fractions, TG and TC contents were measured as described previously.

RNA isolation, cDNA synthesis, and real-time PCR

Total RNA was isolated from frozen tissues utilizing TriPure RNA Isolation Reagent (Roche). mRNA was reverse-transcribed, and cDNA was used for quantitative real-time PCR using iQ SYBR-Green Supermix (MyiQ Thermal Cycler; Bio-Rad CFX96, Veenendaal, Netherlands). Melt curve analysis was included to ensure a single PCR product, and expression levels were normalized using the average expression of β -2-microglobulin and *36b4* as housekeeping genes. Primer sequences are listed in the online repository (20).

Histological analysis

Gonadal white adipose tissue and liver tissue were fixed in 4% paraformaldehyde for 24 hours and stored in 70% ethanol until further processing. Tissues were dehydrated, embedded into paraffin, and cut into 5- μ m sections. Paraffin-waxed tissues were dewaxed and dehydrated before staining with Mayers Hematoxylin (Merck, Netherlands) and eosin (Sigma-Aldrich). Adipocyte size was quantified using ImageJ software [National Institutes of Health, Bethesda, MD (21)]. For F4/80 staining, sections were permeabilized (with 0.1% Tween/PBS), endogenous peroxidases were quenched, and antigens were retrieved with proteinase-K before incubation with a primary F4/80 antibody [1/600; Serotec, Oxford, United Kingdom; RRID: [AB_2098196](https://identifiers.org/AB_2098196) (22)] overnight. Sections were incubated with a goat anti-rat secondary antibody (ImmPRESS™; Vector Laboratories, Peterborough, United Kingdom) for 30 minutes, stained with Nova Red (Vector Laboratories), and counterstained with Mayer Hematoxylin. For Oil Red O staining, frozen hepatic tissue samples were cut in a degreased cryostat at -20°C at 10 μ m. Sections were fixed with formalin, rinsed with isopropanol, stained with filtered Oil Red O working solution (3 g/L; Sigma-Aldrich), counterstained with Mayers Hematoxylin, and mounted with Kaiser glycerol jelly.

RNA sequence analysis

Library construction and RNA sequencing were performed at BGI Tech Solutions CO., LTD (Hong Kong, China). Briefly, isolated RNA was fragmented, and first and second cDNA strands were synthesized. Adapters were ligated to A-tailed mRNA molecules with repaired ends, and cDNA fragments were enriched by PCR amplification and purified for 100-bp paired-end sequencing with the HiSeq 4000 System (HiSeq 3000/4000 SBS Kit; Illumina, Hong Kong, China). All RNA sequence files were processed using the BIOPET Gentrap pipeline version 0.6 developed at the Leiden University Medical Center (http://biopet-docs.readthedocs.io/en/latest/releasenotes/release_notes_0.6.0/). The pipeline includes the processes of quality control (with FastQC version 0.11.2), quality trimming (with Sickle version 1.33), adapter clipping (with Cutadapt version 1.9.1), RNA sequence alignment (with GSNAP version

2014-12-23, with mm10 as reference genome), gene annotation (on 9 November 2015, information was downloaded from the University of California, Santa Cruz Genome Browser), read and base quantification (with HTSeq-count version 0.6.1p1 with settings of “–stranded no”), and low-quality read trimming. After the BIOPET Gentrapp pipeline was run, a differential expression analysis was performed with the edgeR package using R software (23). To correct for multiple testing, the Benjamini and Hochberg false discovery rate was put at 5%. *z* Score data represent the distribution of normalized gene counts across all conditions for genes that showed significant differences between any of the groups. For pathway and mind map analyses, the EuretOS-Knowledge Platform was used. EuretOS allows semantic searches for biologically interesting connections between genes, proteins, metabolites, and drugs based on an underlying database of 176 integrated data sources (January 2017; <http://www.euretOS.com/files/EKPSources2017.pdf>). Data from these databases were obtained in June 2017. Pathway analysis was performed using the Fisher exact test for gene set enrichment.

Statistical analysis

All data are expressed as mean \pm SEM. All *P* values were two-tailed, and *P* < 0.05 was considered statistically significant. Data concerning one factor and two groups were analyzed with an independent sample *t* test. When one factor and more than two groups were investigated, a one-way ANOVA with Fisher *post hoc* test was performed. When the data concerned were both a factor and a time component, a mixed-model analysis was performed in which time was modeled as a factor with less than four time points and as a covariate with four or more time points.

Supplemental materials and data

Supplemental tables and figures can be found in an online repository (20).

Results

CORT118335 prevented obesity and hepatic accumulation of TGs and TC

To evaluate the effect of CORT118335 on obesity and related metabolic parameters, male C57Bl/6J mice received an HFD supplemented with either vehicle (control) or CORT118335 for 3 weeks. CORT118335 significantly attenuated body weight gain (Fig. 1A) caused by a reduction of both fat mass [Fig. 1B; (20)] and lean mass (Fig. 1C). Indirect calorimetry measurements in the first week of treatment showed that CORT118335 treatment reduced caloric intake while increasing energy expenditure and fat oxidation but not carbohydrate oxidation (Fig. 1D–1G). Oral glucose tolerance was improved upon CORT118335 treatment (Fig. 1H). In addition to the overall attenuation of HFD-induced adverse metabolic consequences, CORT118335 elicited a large reduction of hepatic TGs (–59%; *P* < 0.001) and cholesterol (–14%; *P* = 0.02), which was confirmed by Oil Red O staining [Fig. 1I; (20)]. Liver weight was reduced after CORT118335

treatment (20) and so was hepatic inflammation as determined by F4/80 immunostaining (20).

CORT118335 reversed hepatic accumulation of TGs and cholesterol

In view of the substantial change in liver lipid content after CORT118335 treatment, we next evaluated the capacity of CORT118335 to reverse the accumulation of hepatic lipids. Mice received either an LFD, an HFD for 3 or 6 weeks, an HFD with CORT118335 for 6 weeks (“prevention”), or an HFD for 3 weeks followed by an HFD with CORT118335 (“reversal”) (Fig. 1J). CORT118335 treatment attenuated HFD-induced body weight gain in both the prevention and the reversal settings (Fig. 1K). CORT118335 effectively normalized hepatic TG and TC levels to those observed in an LFD in both CORT118335 prevention and reversal treatment groups (Fig. 1L and 1M). Plasma TC levels were increased in CORT118335-treated mice, which was mostly due to an increased high-density lipoprotein fraction (20). To investigate whether CORT118335 reversed liver steatosis in a more severe NAFLD model with noncontinuous drug administration, mice received a 45% HFD for 16 weeks, after which they received CORT118335 treatment via oral gavage for 3 weeks. CORT118335 strongly and dose dependently reduced liver TGs (–41% and –60%; *P* = 0.09 and *P* = 0.009, respectively) (Fig. 1N) but not liver cholesterol (Fig. 1O).

To confirm that selective GR modulation is essential to the improved liver phenotype, the full GR agonist dexamethasone and the full GR antagonist mifepristone were investigated. Both dexamethasone and mifepristone did not improve—and even aggravated—hepatic TG accumulation (20), despite the fact that mifepristone significantly reduced food intake in this experiment (20). This strongly supports the notion that the effects of CORT118335 on hepatic lipid content can be attributed to selective GR modulation.

CORT118335 stimulated hepatic VLDL-TG production

Because liver steatosis develops as a result of an imbalance in hepatic lipid metabolism pathways, expression of genes within these pathways was investigated in vehicle- and CORT118335-treated mice after 3 weeks of treatment. CORT118335 upregulated the expression of genes involved in VLDL production and secretion (*i.e.*, *ApoB*, *Mttp*) but not the expression of genes involved in β -oxidation (*i.e.*, *Cpt1a*, *Acc2*) (Fig. 2A). Genes involved in fatty acid uptake (*i.e.*, *Fabp1*, *Cd36*) were downregulated (Fig. 2A) as were genes involved in *de novo* lipogenesis (*Srebp1c*, *Fasn*, *Dgat2*, *Acc1*) (Fig. 2A). Next, we investigated whether the CORT118335-induced

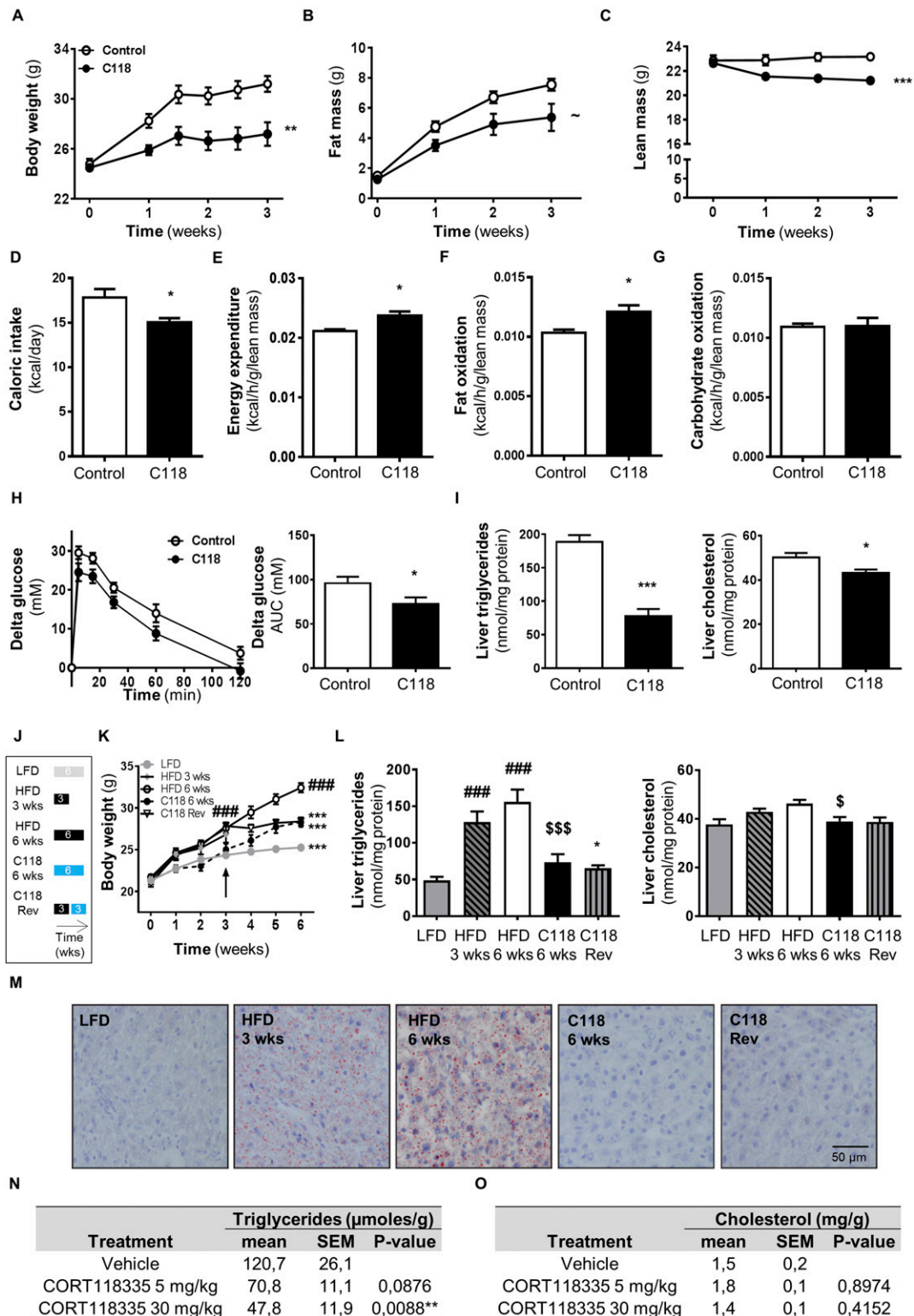


Figure 1. CORT118335 (C118) prevented and reversed hepatic lipid accumulation. In a preventive setting, mice received 10% fructose water and an HFD containing vehicle or C118 for 3 wk ($n = 8$ per group). (A–C) C118 reduced body weight, fat mass, and lean mass. (D–G) C118 additionally reduced caloric intake, energy expenditure, and fat oxidation but not carbohydrate oxidation in week 1. (H) C118 increased intravenous glucose tolerance in week 2; glucose levels shown are corrected for baseline. (I) C118 strongly reduced hepatic TGs and cholesterol levels in week 2. (J) In a reversal (Rev) setting, mice received an LFD, 10% fructose water, and an HFD supplemented with vehicle or C118 or an HFD for 3 wk followed by an HFD supplemented with C118 for 3 wk (Rev; $n = 8$ per group). (K and L) C118 reduced body weight and fully normalized hepatic TG and cholesterol levels. (M) Representative images of hepatic lipid staining using Oil Red O. In a more severe NAFLD model, mice received an HFD for 16 wk after which treatment with vehicle or C118 (5 and 30 mg/kg/d) was started. (N and O) C118 dose dependently reduced hepatic TG levels but not cholesterol level. Scale bar, 50 μm . Data are expressed as mean \pm SEM. $\sim P < 0.1$ vs HFD 3 wk; $*P < 0.05$, $**P < 0.01$, $***P < 0.001$ vs HFD 3 wk; $^{\$}P < 0.05$, $^{\$ \$ \$}P < 0.001$ vs HFD 6 wk; $^{\#\#\#}P < 0.001$ vs LFD. AUC, area under the curve.

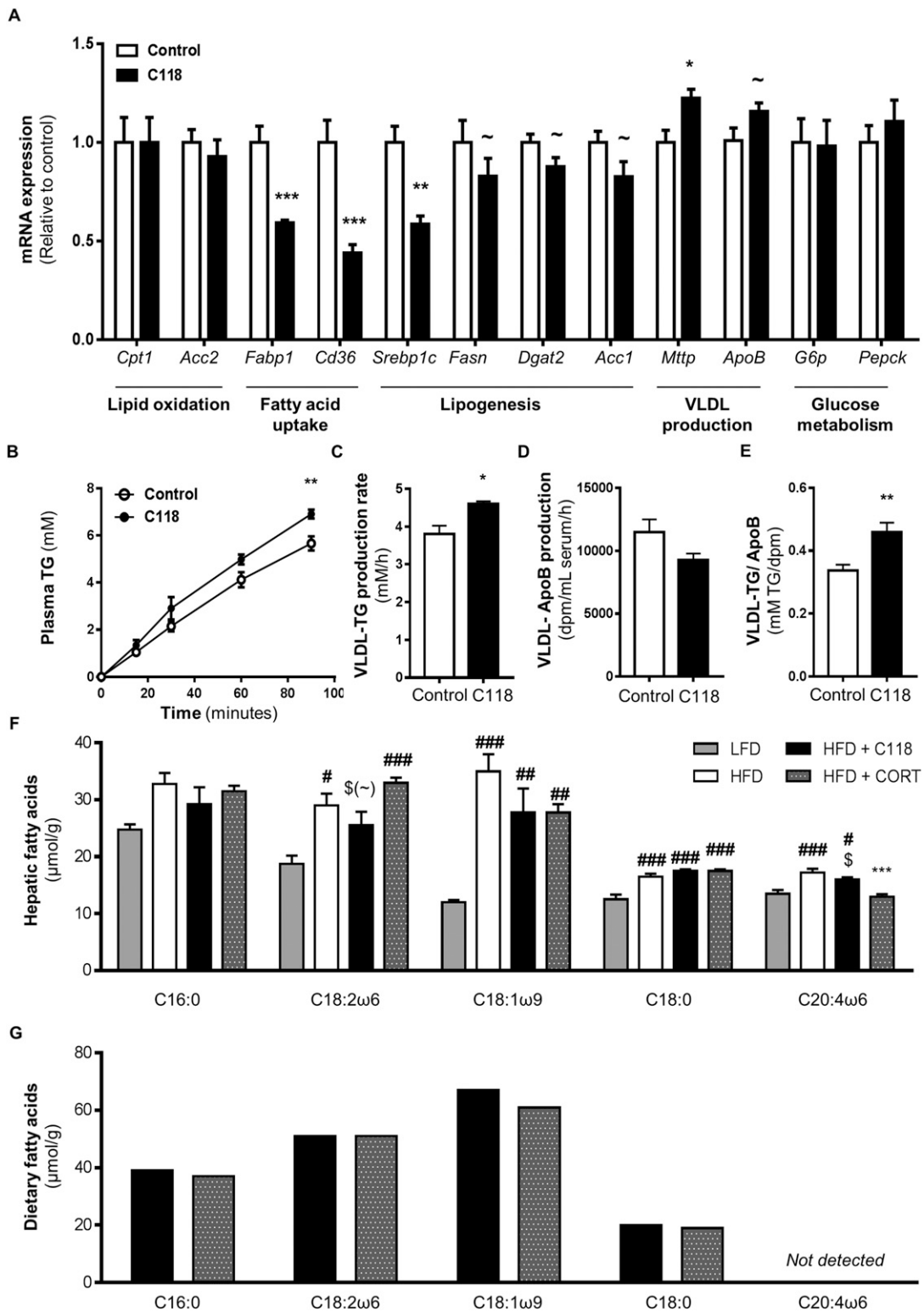


Figure 2. CORT118335 (C118) increased hepatic VLDL-TG production and decreased long-chain fatty acid uptake. (A) In a preventive setting, mice received 10% fructose water with an HFD containing vehicle or C118. C118 selectively affected expression of genes related to hepatic lipid but not to glucose metabolism after 3 wk ($n = 8$ per group). (B and C) VLDL production measurements after 2 d of C118 or vehicle treatment in mice having received HFD for 2.5 wk ($n = 8$ per group) showed that C118 increased plasma TG accumulation after inhibition of tissue lipoprotein lipase (i.e., VLDL-TG production rate). (D and E) The amount of produced VLDL particles was not different as measured with Tran^{35}S labeling of apolipoproteins; CORT118335 rather increased the amount of TG per apoB. (F) Long-chain fatty acid composition indicated C118 reduced fatty acid uptake compared with corticosterone (CORT) treatment (C18:2ω6) but did not alter *de novo* lipogenesis (C20:4ω6). Mice received an LFD, HFD supplemented with vehicle, C118, or CORT for 2 d ($n = 4$ per group) and in (G) respective diets. Data are expressed as mean \pm SEM. $\sim P < 0.1$, $*P < 0.05$, $**P < 0.01$, $***P < 0.001$ vs HFD; $\#P < 0.05$, $\#\#P < 0.01$, $\#\#\#P < 0.001$ vs LFD; $\$(-)P < 0.01$, $\$P < 0.05$ vs CORT.

upregulation of *Mttp* and *ApoB* expression was associated with increased VLDL production by assessing plasma TG accumulation after inhibition of tissue lipoprotein lipase while labeling apolipoproteins with Tran^{35}S . In line with transcriptional data, CORT118335 treatment led to increased plasma TG accumulation over time (Fig. 2B and 2C). Increased hepatic VLDL output involved enhanced lipidation of VLDL particles rather than increased VLDL particle production, as the amount of TGs per apoB, but not plasma apoB, was significantly elevated in CORT118335-treated mice (Fig. 2D and 2E). Because the MTP protein is responsible for the intracellular lipidation of apoB to generate VLDL (24), the upregulation of *Mttp* rather than *ApoB* mRNA appears to be predominantly involved in the biological effect of CORT118335 on VLDL-TG production.

CORT118335 inhibited fatty acid uptake by the liver

We next investigated whether the reduction of fatty acid transporter gene transcription after CORT118335 treatment (Fig. 2A) was accompanied by functional alterations and how these effects were related to receptor (ant)agonism. To this end, long-chain fatty acids (LCFAs) were quantified in the livers of mice after 2 days of treatment with an LFD, HFD, or HFD supplemented with CORT118335 or with corticosterone (Fig. 2F). The essential fatty acid C18:2 ω 6 is a measure for hepatic LCFA uptake, as it is exclusively diet derived and cannot be synthesized *de novo*. CORT118335 tended to reduce hepatic C18:2 ω 6 content compared with content in corticosterone-treated animals, suggesting that CORT118335 decreased hepatic fatty acid uptake. After 6 weeks of CORT118335 treatment, these effects were more pronounced, as hepatic C18:2 ω 6 LCFA levels were fully normalized to LFD levels (20). C20:4 ω 6 LCFA was absent from the diet (Fig. 2G) and therefore reflects elongation of lipids after uptake and *de novo* lipogenesis. Both corticosterone and CORT118335 significantly reduced C20:4 ω 6 content, although the effect of corticosterone was larger (Fig. 2F).

CORT118335 combined partial GR agonistic and antagonistic properties

To identify the early beneficial transcriptional effects of CORT118335, we performed whole transcriptome analysis on livers of mice after 2 days of treatment with an LFD, HFD, or HFD supplemented with CORT118335 or with corticosterone. The overall gene expression profiles of corticosterone- and CORT118335-treated mice were comparable, as well as those of HFD and LFD groups (Fig. 3A). In an HFD condition, corticosterone regulated roughly twice as many genes as CORT118335 (Fig. 3B). Most CORT118335-regulated genes were also regulated

by corticosterone (Fig. 3C). Comparison of gene induction by corticosterone and CORT118335 indicated that despite the higher dosage of CORT118335 and similar K_d , the latter acted as a partial GR agonist with an intrinsic efficacy of 0.65, as calculated from the slope of the regression line (Fig. 3D). Examples of partial agonistic actions of CORT118335 include the upregulation of classical GR target genes *Per1* and *Fkbp5* and recently identified hepatic GR target genes *As3mt* and *Herpud1* (25) after CORT118335 treatment (20). Other genes were strongly regulated by corticosterone but not, or to a much lesser extent, by CORT118335 (Fig. 3D). Expression of GR target genes *Mt1*, *Mt2*, *Abi1*, and *Comt* (25) clearly demonstrated lack of agonism of the compound (20). Partial agonism of CORT118335 on the GR was also evident from effects on *in vivo* hypothalamic-pituitary-adrenal axis dynamics, as the compound suppressed both basal and stress-induced endogenous corticosterone and ACTH plasma levels and reduced tissue weights of the GC-sensitive thymus, adrenals, and spleen (20).

Corticosterone and CORT118335 differentially regulated lipid transport, cholesterol biosynthesis, and cytokine-signaling pathways

Because the beneficial effects of CORT118335 can most likely be attributed to a combination of both GR agonism (*e.g.*, VLDL production) and antagonism (*e.g.*, fatty acid transport), we performed pathway analyses on shared and differentially regulated genes by corticosterone and CORT118335. Shared upregulated genes (20) were enriched for lipid, lipoprotein, glucose, and glycogen metabolism pathways (20). Further subdivision of the “lipid metabolism” pathway showed that both corticosterone and CORT118335 upregulated gene expression for *de novo* lipogenesis and β -oxidation (20). As expected, genes involved in the VLDL production pathway, *Mttp* and *Apob*, were upregulated after both treatments (20).

Differentially expressed genes between corticosterone and CORT118335 ($n = 349$) (Fig. 3B) showed significant enrichment of the “metabolism of lipids and lipoproteins pathway” (Fig. 4A). The genes selectively upregulated by corticosterone but not by CORT118335 were also enriched for lipid metabolism pathways (20), and some genes in this pathway were likely directly regulated by the GR [*Fabp4* (26), *Cd36/FAT* (27–30), and *Nr1h4* (27, 28, 30–32)] (Fig. 4B). Several selectively corticosterone-upregulated genes are associated with liver steatosis [*Cd36/FAT* (33–37), *Nr1h4* (37–39), and *Fabp4* (40, 41)] (Fig. 4B and 4C), and lipid transport [*Cd36/FAT* (42) and *Fabp4* (43)]. Of note, corticosterone, but not CORT118335, also upregulated genes of cholesterol biosynthesis pathways (20). Among these differently regulated

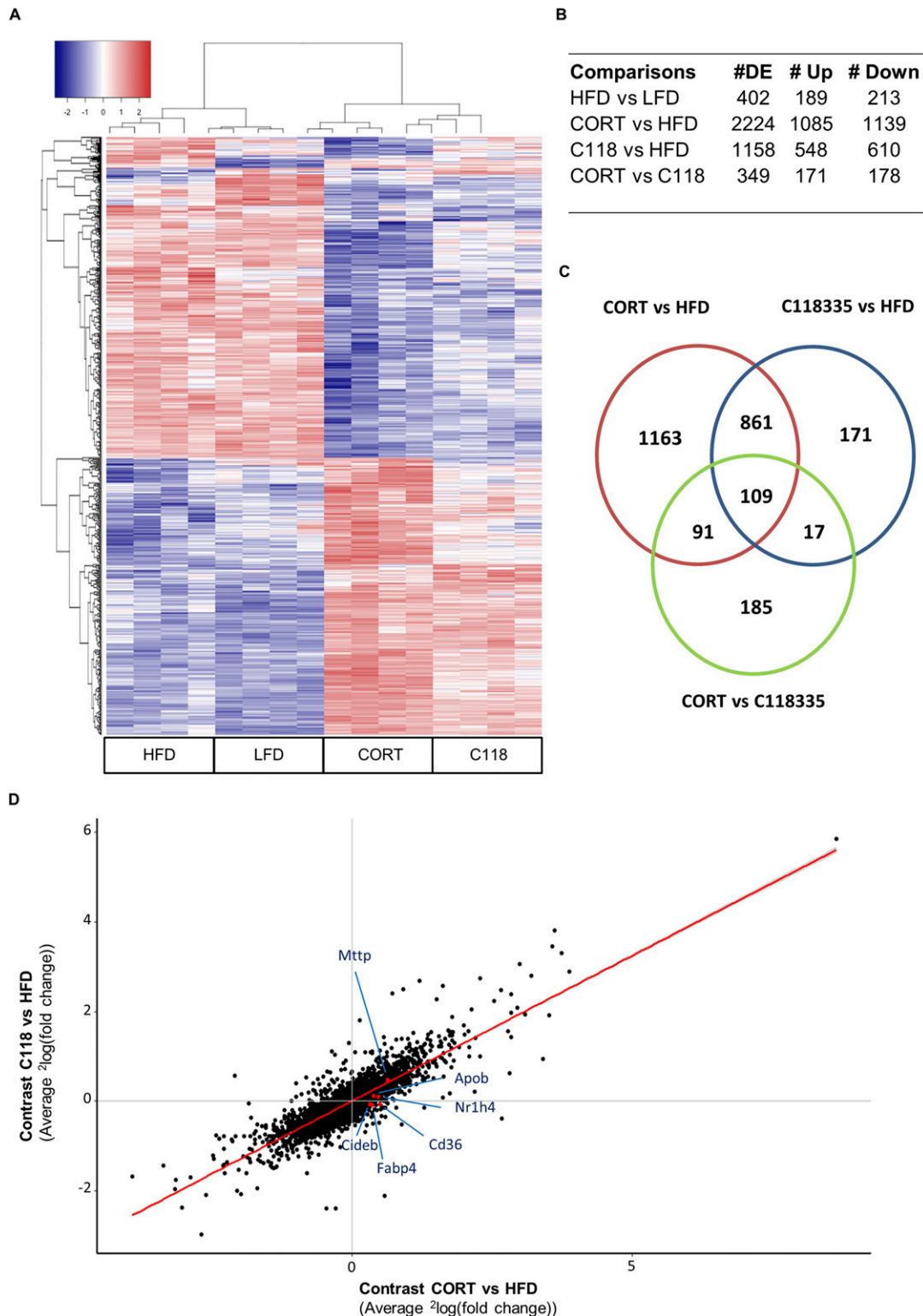
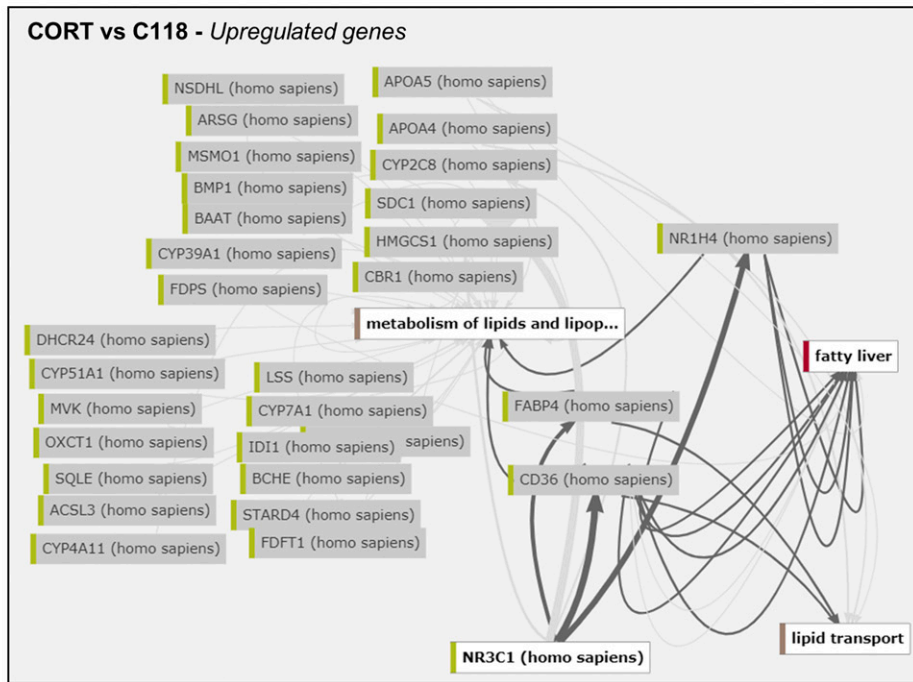


Figure 3. CORT118335 (C118) is a selective GR modulator with predominantly partial agonistic properties on hepatic gene expression. RNA sequence analysis was performed on livers of mice that received an LFD, or 10% fructose water with an HFD supplemented with vehicle, C118, or corticosterone (CORT) for 2 d ($n = 4$ per group). (A) Heatmap of clustered z scores based on the fit to the distribution of normalized gene counts across all conditions for genes that showed significant ($P < 0.00001$) differences between any of the groups. (B) The number of differentially expressed (DE) genes in four different comparisons—(i) HFD vs LFD diet, (ii) CORT vs HFD, (iii) C118 vs HFD, and (iv) CORT vs C118—reveals that C118 regulated half as many genes as CORT. (C) Venn diagram of overlap of upregulated and downregulated genes between different comparisons. (D) The slope of the average log fold-change induction by C118 vs CORT indicates an intrinsic efficacy of 0.65 for most genes, but one that is substantially lower for some genes.

A

Pathway name	Number of genes	P-value
Metabolism of lipids and lipoproteins	41	5,99E-17
Cholesterol biosynthetic process	14	3,35E-14
Superpathway of cholesterol biosynthesis	11	6,03E-13
Biological oxidations	20	5,22E-12
Phase 1 - functionalization of compounds	14	7,55E-11

B



C

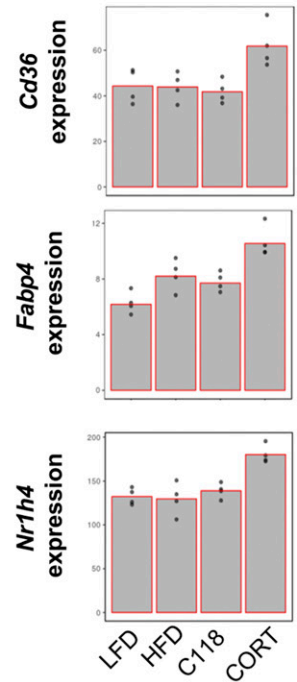


Figure 4. Corticosterone (CORT) but not CORT118335 (C118) upregulated expression of genes involved in hepatic fatty acid uptake. RNA sequence analysis was performed on livers of mice that received an LFD, or 10% fructose water with an HFD supplemented with vehicle, C118, or CORT for 2 d ($n = 4$ per group). (A) Pathway analysis on differentially expressed genes in the CORT vs C118 comparison indicate that CORT regulated lipid metabolism–related genes more strongly than C118 in an HFD context. (B) Relationships between upregulated genes within the “metabolism of lipids and lipoprotein” (metabolism of lipids and lipop...) pathway and “fatty liver,” “*Nr3c1*” (GR gene), and “lipid transport.” (C) Hepatic expression of candidate genes.

genes was *Hmgcs1*, which encodes for one of the rate-limiting enzymes in cholesterol biosynthesis and is a direct target gene of the GR (20, 27, 28, 30, 31). To investigate the effects of CORT118335 on GR-mediated transrepression mechanisms, pathway analysis was performed on genes that were specifically downregulated by corticosterone but not by CORT118335. This revealed that corticosterone but not CORT118335 downregulated “cytokine signaling in immune system” and “Jak-stat signaling” pathways (20).

Discussion

Our data firmly demonstrated that CORT118335 prevents and reverses liver steatosis in mice. To support daily activity and adaptation to stress, endogenous GCs are known to increase the flux of hepatic lipids by increasing VLDL production as well as lipid uptake (44, 45), effects that are predominantly GR mediated (18) (Fig. 5).

CORT118335 selectively recapitulates the lipid outflow component via GR agonism while lacking lipid uptake–promoting activities, altogether confirming its selective GR modulatory profile (13) (Fig. 5). Our transcriptome analysis (early during intervention) showed predominant partial GR agonism in the liver, with some notable exceptions that are likely—and fortuitously—linked to prevention of hepatic lipid accumulation. The major factors involved in reduced hepatic lipid accumulation upon CORT118335 treatment are increased VLDL-TG production, reduced LCFA uptake, and potentially also increased whole-body fatty acid oxidation, as increased fatty acid oxidation in extrahepatic tissues may reduce lipid flux toward the liver. In addition, reduced food intake, adiposity, and *de novo* lipogenesis may contribute to the steatosis-reducing activities of CORT118335. The fact that mifepristone led to a comparable reduction in food intake in most experiments excludes this factor as

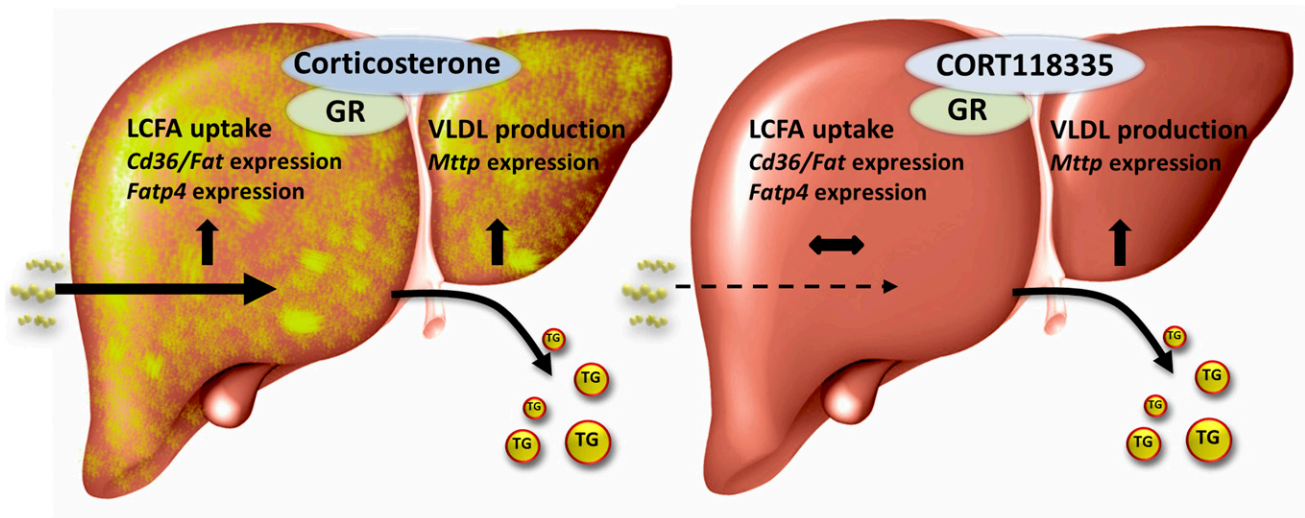


Figure 5. Graphical abstract. Solid arrows indicate large fluxes of TGs, and dashed arrows indicate small fluxes.

the sole responsible mechanism. In this respect, pair feeding experiments can be of interest but were not performed because food restriction is intrinsically stressful and would have strongly complicated our experimental results. In addition to its strong beneficial effects on the liver, CORT118335 treatment also improved overall metabolic health, which is exemplified by a reduction in body weight and improved glucose tolerance, reflecting increased insulin sensitivity. These effects are not unique to CORT118335, as other selective GR modulators, such as CORT108297 and the GR antagonist mifepristone, were shown to have similar metabolic activities (46, 47). The robust effect of CORT118335 on liver lipids is distinctive from that of other GR ligands. Nevertheless, metabolic effects of CORT118335 may be a consequence of reduced hepatic lipid content, thereby improving insulin sensitivity and reducing inflammation (48). Because transcriptome analysis showed that CORT118335 was less capable than corticosterone in transrepressing inflammatory pathways, it is unlikely that CORT118335 is a strong anti-inflammatory drug via classic GR-mediated transrepression (49). The effects of CORT118335 on muscle (and bone) catabolism, as apparent from lean mass data, are most likely driven by (partial) GR agonistic actions and will be the focus of further investigation.

Although extrahepatic mechanisms may contribute to the effects of CORT118335, several facts argue for a strong direct effect on hepatocytes. Measurements of VLDL-TG production, hepatic LCFA composition, and the CORT118335-associated transcriptome were obtained very early after initiation of treatment, even before any substantial (diet-induced) differences in total liver lipid content had developed. In addition, the compound provokes a number of effects that have been found by the specific targeting of liver GR and very short-term

transcriptional changes (25). The substantial body of data on liver lipids based on targeted GR manipulation also argues against a dominant role of the mineralocorticoid receptor, at which CORT118335 acts as a lower affinity antagonist (14). Thus, some liver-specific effects are exclusive for CORT118335 and do reduce NAFLD development.

Although full GR agonism stimulates lipid flux and full GR antagonism lowers lipid flux through the liver, neither leads to hepatic lipid depletion. Our transcriptome analysis supports the concept that the unique combination of partial agonism and antagonism at the GR is responsible for the beneficial liver activities of CORT118335. Corticosterone but not CORT118335 upregulated gene expression of two of six known fatty acid transport proteins that are related to liver influx: *Cd36/Fat* and *Fatp4*. The involvement of CD36/FAT in liver steatosis has been shown, as hepatocyte-specific CD36/FAT knockout mice were protected against HFD-induced hepatic lipid accumulation (36).

In addition to reducing hepatic TGs, CORT118335 had cholesterol-lowering activity. This effect seems to be the result of enhanced cholesterol efflux (VLDL production) and, as suggested from our transcriptomics data, a lack of effect on cholesterol biosynthesis pathways (e.g., *Hmgcs1*). Reducing hepatic cholesterol levels with, for example, HMG-coA inhibitors (statins) was shown to improve NAFLD and nonalcoholic steatohepatitis and was recently even suggested as a novel therapeutic strategy (50, 51).

Selective GR modulation or “dissociated signaling” has been pursued as an inflammatory disease treatment for decades (52). Our data establish that it is feasible to use selective GR modulation to target GR-dependent diseases by interfering with metabolic fluxes—not only

in prevention but also in a reversal setting. Further mechanistic studies on selective receptor modulators will enhance understanding and help predict which GR transcriptional coregulators and signaling pathways are involved in pathogenic processes. By itself, CORT118335 forms an interesting lead for future clinical development.

Acknowledgments

We gratefully thank Sander van der Zeeuw for valuable assistance with bioinformatics analysis of the A sequence data. We also thank our colleagues at RenaSci (Nottingham) for conducting mouse experiments that were of great value to the manuscript.

Financial Support: This study was partially funded by Corcept Therapeutics. L.L.K. was funded with a grant from the Board of Directors of Leiden University Medical Center. K.M.H. was supported by the European Community's Seventh Framework Programme (FP7/2007-2013) under grant agreement no. 305444 "RD-Connect."

Correspondence: Onno C. Meijer, PhD, Department of Internal Medicine, Division of Endocrinology, Leiden University Medical Center, Room C7-44, 2333 ZA Leiden, Netherlands. E-mail: o.c.meijer@lumc.nl.

Disclosure Summary: H.H. and J.K.B. are employees of Corcept Therapeutics, a pharmaceutical company that develops selective modulators, including CORT118335. K.M.H. performs paid consultancy for Euretos b.v., a startup that develops knowledge management and discovery services for the life sciences with the Euretos Knowledge Platform as a marketed product. CORT118335 has been filed for a patent (WO2012/129074), for which J.K.v.d.H. and O.C.M. are co-inventors. The remaining authors have nothing to disclose.

References

- Blachier M, Leleu H, Peck-Radosavljevic M, Valla DC, Roudot-Thoraval F. The burden of liver disease in Europe: a review of available epidemiological data. *J Hepatol*. 2013;58(3):593–608.
- Rinella ME, Sanyal AJ. Management of NAFLD: a stage-based approach. *Nat Rev Gastroenterol Hepatol*. 2016;13(4):196–205.
- Vernon G, Baranova A, Younossi ZM. Systematic review: the epidemiology and natural history of non-alcoholic fatty liver disease and non-alcoholic steatohepatitis in adults. *Aliment Pharmacol Ther*. 2011;34(3):274–285.
- Woods CP, Hazlehurst JM, Tomlinson JW. Glucocorticoids and non-alcoholic fatty liver disease. *J Steroid Biochem Mol Biol*. 2015;154:94–103.
- Hollenberg SM, Weinberger C, Ong ES, Cerelli G, Oro A, Lebo R, Thompson EB, Rosenfeld MG, Evans RM. Primary structure and expression of a functional human glucocorticoid receptor cDNA. *Nature*. 1985;318(6047):635–641.
- Yu CY, Mayba O, Lee JV, Tran J, Harris C, Speed TP, Wang JC. Genome-wide analysis of glucocorticoid receptor binding regions in adipocytes reveal gene network involved in triglyceride homeostasis. *PLoS One*. 2010;5(12):e15188.
- Vegiopoulos A, Herzig S. Glucocorticoids, metabolism and metabolic diseases. *Mol Cell Endocrinol*. 2007;275(1-2):43–61.
- D'souza AM, Beaudry JL, Sziagiato AA, Trumble SJ, Snook LA, Bonen A, Giacca A, Riddell MC. Consumption of a high-fat diet rapidly exacerbates the development of fatty liver disease that occurs with chronically elevated glucocorticoids. *Am J Physiol Gastrointest Liver Physiol*. 2012;302(8):G850–G863.
- Warrier M, Hinds TD Jr, Ledford KJ, Cash HA, Patel PR, Bowman TA, Stechschulte LA, Yong W, Shou W, Najjar SM, Sanchez ER. Susceptibility to diet-induced hepatic steatosis and glucocorticoid resistance in FK506-binding protein 52-deficient mice. *Endocrinology*. 2010;151(7):3225–3236.
- Asagami T, Belanoff JK, Azuma J, Blasey CM, Clark RD, Tsao PS. Selective glucocorticoid receptor (GR-II) antagonist reduces body weight gain in mice. *J Nutr Metab*. 2011;2011:235389.
- Thiele S, Ziegler N, Tsourdi E, De Bosscher K, Tuckermann JP, Hofbauer LC, Rauner M. Selective glucocorticoid receptor modulation maintains bone mineral density in mice. *J Bone Miner Res*. 2012;27(11):2242–2250.
- Brandish PE, Anderson K, Baltus GA, Bai C, Bungard CJ, Bunting P, Byford A, Chiu CS, Cicmil M, Corcoran H, Euler D, Fisher JE, Gambone C, Hasbun-Manning M, Kuklin N, Landis E, Lifested TQ, McElwee-Witmer S, McIntosh IS, Meissner RS, Miao J, Mitchell HJ, Musselman A, Schmidt A, Shin J, Szczerba P, Thompson CD, Tribouley C, Vogel RL, Warrier S, Hershey JC. The preclinical efficacy, selectivity and pharmacologic profile of MK-5932, an insulin-sparing selective glucocorticoid receptor modulator. *Eur J Pharmacol*. 2014;724:102–111.
- Atucha E, Zalachoras I, van den Heuvel JK, van Weert LT, Melchers D, Mol IM, Belanoff JK, Houtman R, Hunt H, Roozendaal B, Meijer OC. A mixed glucocorticoid/mineralocorticoid selective modulator with dominant antagonism in the male rat brain. *Endocrinology*. 2015;156(11):4105–4114.
- Hunt HJ, Ray NC, Hynd G, Sutton J, Sajad M, O'Connor E, Ahmed S, Lockett P, Daly S, Buckley G, Clark RD, Roe R, Blasey C, Belanoff J. Discovery of a novel non-steroidal GR antagonist with in vivo efficacy in the olanzapine-induced weight gain model in the rat. *Bioorg Med Chem Lett*. 2012;22(24):7376–7380.
- Zalachoras I, Houtman R, Atucha E, Devos R, Tijssen AM, Hu P, Lockett PM, Datson NA, Belanoff JK, Lucassen PJ, Joëls M, de Kloet ER, Roozendaal B, Hunt H, Meijer OC. Differential targeting of brain stress circuits with a selective glucocorticoid receptor modulator. *Proc Natl Acad Sci USA*. 2013;110(19):7910–7915.
- Van Klinken JB, van den Berg SA, Havekes LM, Willems Van Dijk K. Estimation of activity related energy expenditure and resting metabolic rate in freely moving mice from indirect calorimetry data. *PLoS One*. 2012;7(5):e36162.
- Redgrave TG, Roberts DC, West CE. Separation of plasma lipoproteins by density-gradient ultracentrifugation. *Anal Biochem*. 1975;65(1-2):42–49.
- Bligh EG, Dyer WJ. A rapid method of total lipid extraction and purification. *Can J Biochem Physiol*. 1959;37(8):911–917.
- Muskiet FA, van Doormaal JJ, Martini IA, Wolthers BG, van der Slik W. Capillary gas chromatographic profiling of total long-chain fatty acids and cholesterol in biological materials. *J Chromatogr A*. 1983;278(2):231–244.
- Koorneef LL, Heuvel JKvd, Kroon J, Boon MR, Hoen PAct, Hettne KM, Velde NMvd, Kolenbrander KB, Streefland TCM, Mol IM, Sips HCM, Kielbasa SM, Mei H, Belanoff JK, Pereira AM, Oosterveer MH, Hunt H, Rensen PCN, Meijer OC. Data from: Selective glucocorticoid receptor modulation prevents and reverses nonalcoholic fatty liver disease in male mice. figshare 2018. Deposited 20 September 2018. <https://dx.doi.org/10.6084/m9.figshare.7110815>.
- Schneider CA, Rasband WS, Eliceiri KW. NIH Image to ImageJ: 25 years of image analysis. *Nat Methods*. 2012;9(7):671–675.
- RRID:AB_2098196.
- McCarthy DJ, Chen Y, Smyth GK. Differential expression analysis of multifactor RNA-seq experiments with respect to biological variation. *Nucleic Acids Res*. 2012;40(10):4288–4297.
- Shelness GS, Sellers JA. Very-low-density lipoprotein assembly and secretion. *Curr Opin Lipidol*. 2001;12(2):151–157.

25. Phuc Le P, Friedman JR, Schug J, Brestelli JE, Parker JB, Bochkis IM, Kaestner KH. Glucocorticoid receptor-dependent gene regulatory networks. *PLoS Genet.* 2005;1(2):e16.
26. Davis AP, Grondin CJ, Johnson RJ, Sciaky D, King BL, McMorran R, Wiegiers J, Wiegiers TC, Mattingly CJ. The Comparative Toxicogenomics Database: update 2017. *Nucleic Acids Res.* 2017;45(D1):D972–D978.
27. Cerami EG, Gross BE, Demir E, Rodchenkov I, Babur O, Anwar N, Schultz N, Bader GD, Sander C. Pathway Commons, a web resource for biological pathway data. *Nucleic Acids Res.* 2011;39(Suppl 1):D685–D690.
28. Wingender E. The TRANSFAC project as an example of framework technology that supports the analysis of genomic regulation. *Brief Bioinform.* 2008;9(4):326–332.
29. Orchard S, Ammari M, Aranda B, Breuza L, Briganti L, Broackes-Carter F, Campbell NH, Chavali G, Chen C, del-Toro N, Duesbury M, Dumousseau M, Galeota E, Hinz U, Iannuccelli M, Jagannathan S, Jimenez R, Khadake J, Lagreid A, Licata L, Lovering RC, Meldal B, Melidoni AN, Milagros M, Peluso D, Perfetto L, Porras P, Raghunath A, Ricard-Blum S, Roehert B, Stutz A, Tognolli M, van Roey K, Cesareni G, Hermjakob H. The MIntAct project—IntAct as a common curation platform for 11 molecular interaction databases. *Nucleic Acids Res.* 2014;42(D1):D358–D363.
30. Chatr-aryamontri A, Oughtred R, Boucher L, Rust J, Chang C, Kolas NK, O'Donnell L, Oster S, Theesfeld C, Sellam A, Stark C, Breitkreutz BJ, Dolinski K, Tyers M. The BioGRID interaction database: 2017 update. *Nucleic Acids Res.* 2017;45(D1):D369–D379.
31. Fabregat A, Sidiropoulos K, Garapati P, Gillespie M, Hausmann K, Haw R, Jassal B, Jupe S, Korninger F, McKay S, Matthews L, May B, Milacic M, Rothfels K, Shamovsky V, Webber M, Weiser J, Williams M, Wu G, Stein L, Hermjakob H, D'Eustachio P. The Reactome pathway Knowledgebase. *Nucleic Acids Res.* 2016;44(D1):D481–D487.
32. Milacic M, Haw R, Rothfels K, Wu G, Croft D, Hermjakob H, D'Eustachio P, Stein L. Annotating cancer variants and anti-cancer therapeutics in reactome. *Cancers (Basel).* 2012;4(4):1180–1211.
33. Declercq J, Brouwers B, Pruniau VP, Stijnen P, de Faudeur G, Tuand K, Meulemans S, Serneels L, Schraenen A, Schuit F, Creemers JW. Metabolic and behavioural phenotypes in Nestin-Cre mice are caused by hypothalamic expression of human growth hormone. *PLoS One.* 2015;10(8):e0135502.
34. Yao L, Wang C, Zhang X, Peng L, Liu W, Zhang X, Liu Y, He J, Jiang C, Ai D, Zhu Y. Hyperhomocysteinemia activates the aryl hydrocarbon receptor/CD36 pathway to promote hepatic steatosis in mice. *Hepatology.* 2016;64(1):92–105.
35. Zhou J, Febbraio M, Wada T, Zhai Y, Kuruba R, He J, Lee JH, Khadem S, Ren S, Li S, Silverstein RL, Xie W. Hepatic fatty acid transporter *Cd36* is a common target of LXR, PXR, and PPAR γ in promoting steatosis. *Gastroenterology.* 2008;134(2):556–567.e1.
36. Wilson CG, Tran JL, Erion DM, Vera NB, Febbraio M, Weiss EJ. Hepatocyte-specific disruption of *CD36* attenuates fatty liver and improves insulin sensitivity in HFD-fed mice. *Endocrinology.* 2016;157(2):570–585.
37. Piñero J, Bravo À, Queralt-Rosinach N, Gutiérrez-Sacristán A, Deu-Pons J, Centeno E, García-García J, Sanz F, Furlong LI. DisGeNET: a comprehensive platform integrating information on human disease-associated genes and variants. *Nucleic Acids Res.* 2017;45(D1):D833–D839.
38. Côté I, Ngo Sock ET, Lévy É, Lavoie JM. An atherogenic diet decreases liver FXR gene expression and causes severe hepatic steatosis and hepatic cholesterol accumulation: effect of endurance training. *Eur J Nutr.* 2013;52(5):1523–1532.
39. Martin IV, Schmitt J, Minckenberg A, Mertens JC, Stieger B, Mullhaupt B, Geier A. Bile acid retention and activation of endogenous hepatic farnesoid-X-receptor in the pathogenesis of fatty liver disease in ob/ob-mice. *Biol Chem.* 2010;391(12):1441–1449.
40. Graupera I, Coll M, Pose E, Elia C, Piano S, Solà E, Blaya D, Huelin P, Solé C, Moreira R, de Prada G, Fabrellas N, Juanola A, Morales-Ruiz M, Sancho-Bru P, Villanueva C, Ginès P. Adipocyte fatty-acid binding protein is overexpressed in cirrhosis and correlates with clinical outcomes. *Sci Rep.* 2017;7(1):1829.
41. Masetti M, Bianchi G, Gianotti G, Giovagnoli M, Vizioli L, Zorzi V, Rossi V, Forti P, Zoli M. Adipocyte-fatty acid binding protein and non-alcoholic fatty liver disease in the elderly. *Aging Clin Exp Res.* 2014;26(3):241–247.
42. Jeppesen J, Mogensen M, Prats C, Sahlin K, Madsen K, Kiens B. FAT/CD36 is localized in sarcolemma and in vesicle-like structures in subsarcolemma regions but not in mitochondria. *J Lipid Res.* 2010;51(6):1504–1512.
43. Schaefer CF, Anthony K, Krupa S, Buchoff J, Day M, Hannay T, Buetow KH. PID: the Pathway Interaction Database. *Nucleic Acids Res.* 2009;37(Suppl 1):D674–D679.
44. van den Beukel JC, Boon MR, Steenbergen J, Rensen PC, Meijer OC, Themmen AP, Grefhorst A. Cold exposure partially corrects disturbances in lipid metabolism in a male mouse model of glucocorticoid excess. *Endocrinology.* 2015;156(11):4115–4128.
45. Spiga F, Walker JJ, Terry JR, Lightman SL. HPA axis-rhythms. *Compr Physiol.* 2014;4(3):1273–1298.
46. van den Heuvel JK, Boon MR, van Hengel I, Peschier-van der Put E, van Beek L, van Harmelen V, van Dijk KW, Pereira AM, Hunt H, Belanoff JK, Rensen PC, Meijer OC. Identification of a selective glucocorticoid receptor modulator that prevents both diet-induced obesity and inflammation. *Br J Pharmacol.* 2016;173(11):1793–1804.
47. Mammi C, Marzolla V, Armani A, Feraco A, Antelmi A, Maslak E, Chlopicki S, Cinti F, Hunt H, Fabbri A, Caprio M. A novel combined glucocorticoid-mineralocorticoid receptor selective modulator markedly prevents weight gain and fat mass expansion in mice fed a high-fat diet. *Int J Obes.* 2016;40(6):964–972.
48. Lonardo A, Lombardini S, Ricchi M, Scaglioni F, Loria P. Review article: hepatic steatosis and insulin resistance. *Aliment Pharmacol Ther.* 2005;22(s2):64–70.
49. De Bosscher K, Van Craenenbroeck K, Meijer OC, Haegeman G. Selective transrepression versus transactivation mechanisms by glucocorticoid receptor modulators in stress and immune systems. *Eur J Pharmacol.* 2008;583(2-3):290–302.
50. Imprialos KP, Stavropoulos K, Doumas M, Skalkou A, Zografou I, Athyros VG. The potential role of statins in treating liver disease. *Expert Rev Gastroenterol Hepatol.* 2018;12(4):331–339.
51. Seif El-Din SH, El-Lakkany NM, El-Naggar AA, Hammam OA, Abd El-Latif HA, Ain-Shoka AA, Ebeid FA. Effects of rosuvastatin and/or β -carotene on non-alcoholic fatty liver in rats. *Res Pharm Sci.* 2015;10(4):275–287.
52. Sundahl N, Bridelance J, Libert C, De Bosscher K, Beck IM. Selective glucocorticoid receptor modulation: new directions with non-steroidal scaffolds. *Pharmacol Ther.* 2015;152:28–41.